Title	Stationary and adaptive color-shift reduction methods based on the bilevel driving technique for phosphor-converted white LEDs
Author(s)	Loo, KH; Lai, YM; Tan, SC; Tse, CK
Citation	IEEE Transactions on Power Electronics, 2011, v. 26 n. 7, p. 1943-1953
Issued Date	2011
URL	http://hdl.handle.net/10722/155641
Rights	©2011 IEEE. Personal use of this material is permitted. However, permission to reprint/republish this material for advertising or promotional purposes or for creating new collective works for resale or redistribution to servers or lists, or to reuse any copyrighted component of this work in other works must be obtained from the IEEE.

Stationary and Adaptive Color-Shift Reduction Methods Based on the Bilevel Driving Technique for Phosphor-Converted White LEDs

K. H. Loo, Y. M. Lai, Siew-Chong Tan, and Chi K. Tse

***Abstract*—The bilevel driving technique has realized a 2-D control of the luminosity and emitted color of white LEDs with duty cycle and forward current levels. Unfortunately, various combinations of these dimming control parameters can lead to significant changes in junction temperature, which further modify the luminosity and emitted color of LEDs. In this paper, the theoretical aspects of these complex interactions and the impact of bilevel drive on the color-shift properties of white LEDs are discussed in detail by using a mathematical color-shift model. Two color-shift reduction methods are proposed based on the insights obtained from this model. This study shows that a heat sink's thermal resistance that minimizes the overall color shift over dimming can be uniquely determined from the knowledge of some measurable LED parameters, and gives rise to a global minimum color shift. If such a thermal resistance cannot be realized due to practical limitations, the second method that utilizes an adaptive change of forward current levels over dimming can be adopted. Based on their nature, these methods are classified as stationary and adaptive methods, respectively. Their validity is supported by experimental measurements on a commercial white LED.**

***Index Terms*—Color control, driving method, LED color, light-emitting diode (LED), white LED.**

I. Introduction

WHITE light-emitting diodes (white LEDs) based on phosphor conversion of blue LEDs have attracted a significant degree of attention since the last decade as a potential substitution for conventional, century-old white light sources including incandescent and fluorescent lamps. In general, on the suitability for dimming, conventional light sources based on heated filament commonly suffer from a major drawback that a minimum surface temperature must be maintained at the lamp's filament for proper operation [1]; hence, a full-range continuous dimming is typically not possible. For example, incandescent lamps can only be dimmed to a minimum temperature below which the tungsten filament will mostly emit infrared light that is invisible to human eyes and the lamp will appear to have extinguished. For fluorescent lamps, the filaments at the electrodes must be heated continuously to ensure a sufficient emission of free electrons for maintaining the plasma's conductivity. This is normally achieved by self-heating from the plasma, except when the lamp is dimmed to a very low luminosity during which an external circuitry will be required to provide the heating power to prevent the lamp from extinguishing [2]–[4]. This has increased the complexities and costs of the lamp ballasts designed with a wide dimming range.

In contrast to conventional light sources, the absence of this drawback in solid-state lamps such as white LEDs makes them exceptionally well suited for dimming applications. Once the threshold voltage is exceeded, LEDs can be continuously operated from zero up to the maximum allowable forward current specified by the manufacturers; therefore, a full-range continuous dimming can be achieved by varying the forward current amplitude directly, i.e., amplitude modulation (AM). Since LEDs are capable of responding extremely fast to time-varying currents, they can also be operated by pulsating current where the peak forward current is fixed in amplitude and dimming is achieved by varying the pulse's duty cycle, i.e., pulse width modulation (PWM). From a previous study [5], it has been verified that, among the two methods discussed, a higher luminous output and better color stability over dimming are obtained with AM, but it gives rise to a nonlinear dimming profile due to the saturable luminous output characteristic of LEDs at large forward currents [6]–[9]. Dimming the LEDs with PWM linearizes the dimming profile but at the penalties of lower luminous output and more significant color shift over dimming.

The bilevel driving technique has been proposed recently by the authors to mitigate some of the problems inherent with AM and PWM dimming [10], [11]. It is aimed to improve the luminous output of LEDs by introducing a second current level (dc offset) into the conventional PWM waveform, forming a bilevel current, while the linearity of dimming is maintained by duty-cycle control of the duration of each current level. Technically, the use of two current levels implies that a 2-D dimming is possible with both current levels and duty cycle as the dimming control parameters. With this approach, various combinations of these parameters can give rise to the same required average forward current, but clearly the luminous output and emitted color will vary in each case depending on the specific parameter values being chosen. The impact of bilevel dimming on the luminous performance of white LEDs was discussed in

Manuscript received July 5, 2010; revised September 14, 2010; accepted November 27, 2010. Date of current version August 5, 2011. Recommended for publication by Associate Editor M. Alonso.

K. H. Loo is with the Faculty of Engineering, The Hong Kong Polytechnic University, Kowloon, Hong Kong (e-mail: kh.loo@polyu.edu.hk).

Y. M. Lai, S. C. Tan, and C. K. Tse are with the Department of Electronic and Information Engineering, The Hong Kong Polytechnic University, Kowloon, Hong Kong (e-mail: enymlai@polyu.edu.hk; ensctan@eie.polyu.edu.hk; encktse@eie.polyu.edu.hk).

Color versions of one or more of the figures in this paper are available online at http://ieeexplore.ieee.org.

Digital Object Identifier 10.1109/TPEL.2010.2097610

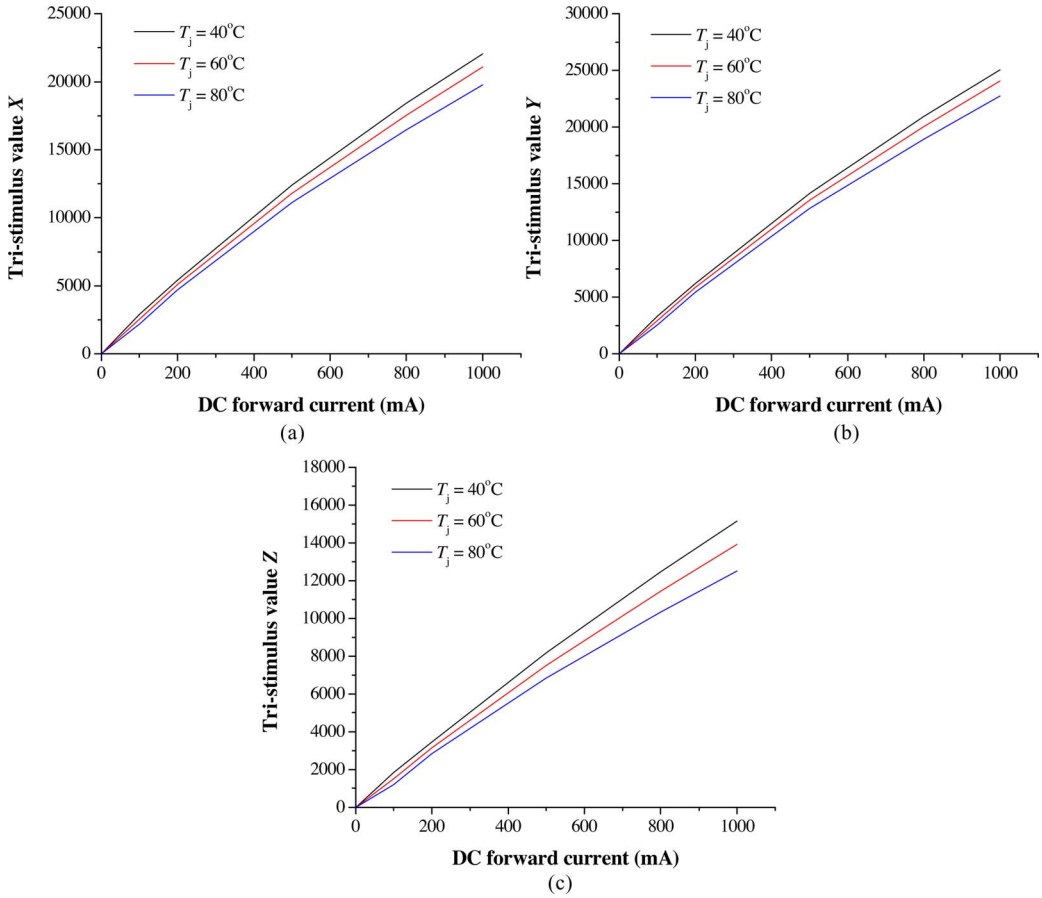

Fig. 1. Tristimulus values [(a) X, (b) Y, (c) Z] measured on a Philips-Lumileds LUXEON K2 (LXK2-PW14-U00, cool white) phosphor-converted white-LED sample under various dc forward currents and junction temperatures.

depth previously [10], [11], but its impact on another important performance indicator, the color stability over dimming, has not been addressed. Due to the strong dependences of the peak-emission-wavelength shift property of white LEDs on the forward current amplitude and junction temperature [12]–[14], their color-stability performance over dimming is anticipated to be a complex function of current levels, duty cycle, and the specific thermal design implemented.

In this paper, we begin with an experimental characterization of the chromaticity properties of white LEDs under various forward current levels and junction temperatures, followed by a theoretical study of the generic color-shift properties of white LEDs under bilevel dimming. The theoretical background related to the impact of this dimming approach on the color stability of white LEDs is discussed by using a simplified mathematical color-shift model to be developed in Section III. The model reveals the two possible approaches, stationary and adaptive, for reducing the overall color shift over dimming by means of a guided selection of heat sink's thermal resistance and current levels. In Section IV, the details of the stationary and adaptive color-shift reduction methods are further developed and experiments are conducted on a commercial white-LED sample to verify the proposed concepts.

II. Characterization of Chromaticity Properties of White LEDs

In this section, an experiment was conducted to observe the color-shift properties of a commercial white LED, LUXEON K2, under the influences of the dc forward current and junction temperature changes. The same experiment was conducted on another white-LED sample, XLAMP XREWHT-L1, produced by CREE and similar observations were found; therefore, the results will not be discussed here to avoid duplication. The measurements were conducted using the experimental setup described in the following. To isolate the effects of forward current level and junction temperature, the LUXEON K2 white-LED sample is mounted on a thermoelectric heater/cooler, acting as an active heat sink, so that the junction temperature can be controlled independently. The heat sink's temperature $T_{\rm hs}$ required to generate a desired junction temperature T_j for a given forward current level I_f can be estimated using the thermal resistance model described by (1), where k_h is the portion of input electrical power $V_f \cdot I_f$ is dissipated as heat. According to this model, for each forward current level, the heat sink's temperature was adjusted to a value estimated from the LED's junction-to-case temperature drop, which, in turn, is determined from the product of the known junction-to-case thermal resistance $R_{j\text{-}c}$ (from

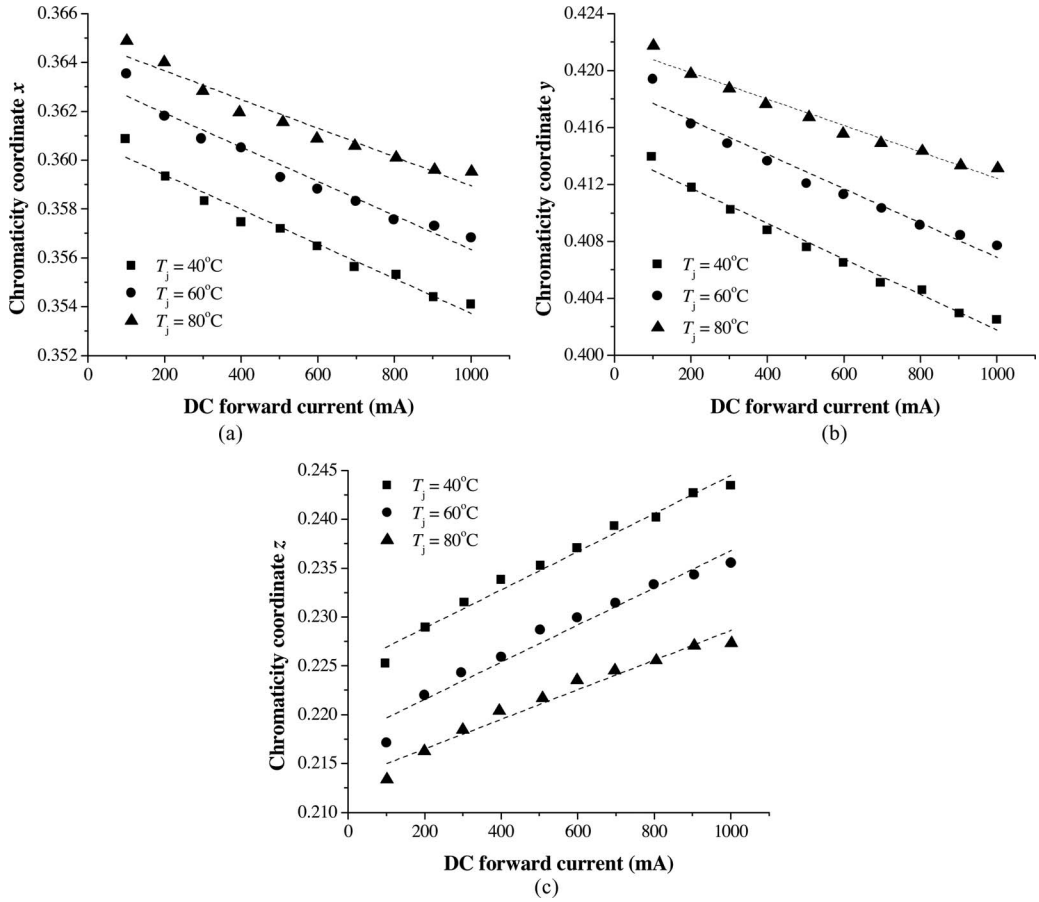

Fig. 2. Chromaticity coordinates [(a) x, (b) y, (c) z] measured on a Philips-Lumileds LUXEON K2 (LXK2-PW14-U00, cool white) phosphor-converted white-LED sample under various dc forward currents. Dashed lines denote linear fits to the experimental data.

datasheet) and the measured forward voltage V_f and current I_f. In general, k_h is not constant but varies nonlinearly with the power level of LED [15]. For LUXEON K2, the measurements in [15] showed that k_h varies gradually from 0.85 to 0.90 for 67–100% of the rated power. Although experimental data are not available for <67% of the rated power, the variation in k_h is expected to be smaller in degree considering that the efficacy "droop" effect is not predominant at small forward currents and the luminous efficacy is approximately constant. Therefore, for the convenience of computation, a constant value of $k_h = 0.85$ is used in this study, but the results are computed based on this assumption and the theory proposed in Section III should be subjected to fine-tuning when implemented in practice. Since thermal paste is used between the LED's case and the heat sink, $R_{c\text{-hs}}$ is assumed to be small compared to the junction-to-case thermal resistance $R_{j\text{-}c}$ of the LED, 9°C/W, specified in the datasheet [16]:

$$\begin{aligned} T_j &= (R_{j\text{-}c} + R_{c\text{-hs}}) \cdot k_h \cdot V_f \cdot I_f + T_{\text{hs}} \\ &\approx R_{j\text{-}c} \cdot k_h \cdot V_f \cdot I_f + T_{\text{hs}}. \end{aligned} \tag{1}$$

For optical measurements, the heat sink and LED assembly are housed inside a closed light chamber (to avoid interference from ambient light), where the emitted light from the LED is detected by a miniature fiber optic spectrometer USB4000 produced by Ocean Optics. The measured tristimulus values X (red), Y (green), and Z (blue) are then used to calculate the chromaticity coordinates (x, y, z) according to $x = X/(X + Y + Z)$, $y = Y/(X + Y + Z)$, and $z = 1 - x - y$, from which the chromaticity coordinates x, y, and z can be viewed as the normalized degree of stimulation of the red, green, and blue cones of human eyes, respectively. In a dichromatic white light, since the degree of stimulation of the red and green cones, x and y, both originate from the phosphor-converted yellow light, they are expected to vary in phase with each other, as verified in Figs. 2 and 3.

From Figs. 2 and 3, one can observe that $\partial x/\partial I_f$ and $\partial y/\partial I_f$ are approximately constant for all junction temperatures, while $\partial x/\partial T_j$ and $\partial y/\partial T_j$ are approximately constant for all forward current levels. For the convenience of computation, they are assumed to be constant and the average values are used in the following discussion:

$$\frac{\partial x}{\partial I_f} \approx -6.64 \times 10^{-3}\text{A}^{-1} \tag{2}$$

$$\frac{\partial y}{\partial I_f} \approx -1.12 \times 10^{-2}\text{A}^{-1} \tag{3}$$

$$\frac{\partial x}{\partial T_j} \approx 1.20 \times 10^{-4}{}^{\circ}\text{C}^{-1} \tag{4}$$

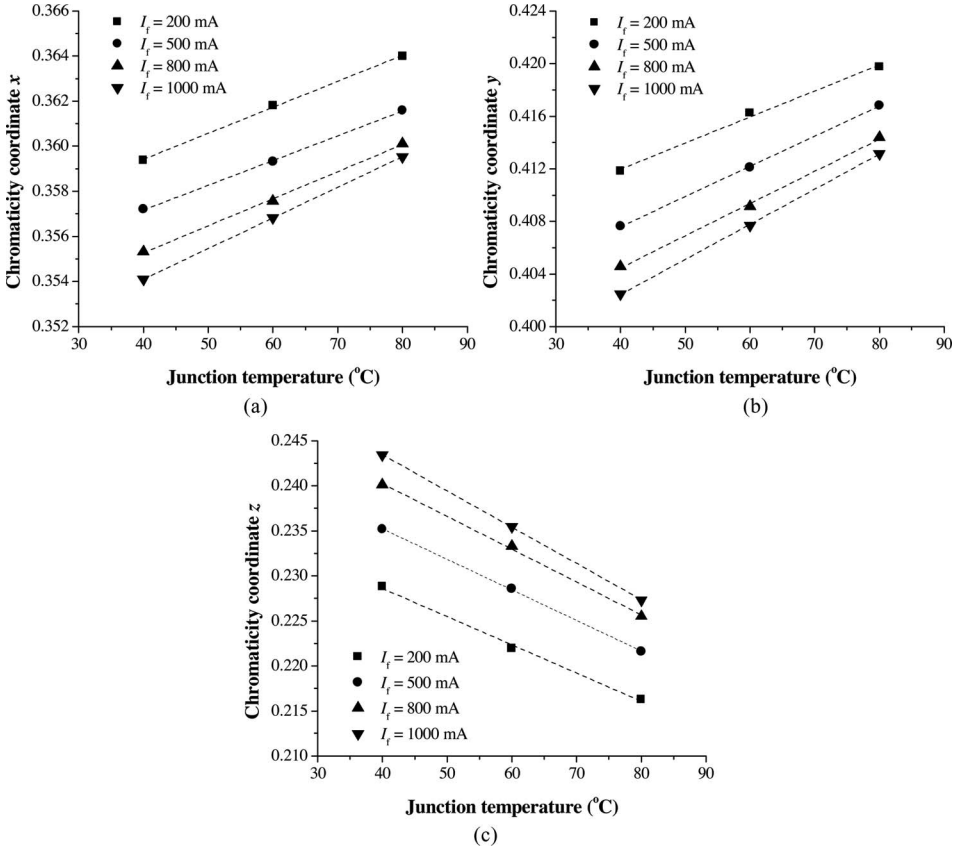

Fig. 3. Chromaticity coordinates [(a) x, (b) y, (c) z] measured on a Philips-Lumileds LUXEON K2 (LXK2-PW14-U00, cool white) phosphor-converted white-LED sample under various junction temperatures. Dashed lines denote linear fits to the experimental data.

$$\frac{\partial y}{\partial T_j} \approx 2.35 \times 10^{-4\circ}\mathrm{C}^{-1}. \tag{5}$$

III. Simplified Color-Shift Model Under Bilevel Drive

In this section, a simplified mathematical color-shift model will be derived for the case when an LED is driven/dimmed by bilevel current. By definition, bilevel current is a PWM-like current that pulsates between a higher current level I_H and a lower nonzero current level I_L, and duty cycle D is the duration of I_H normalized to the pulse repetition time. Mathematically, the average forward current $\overline{I_f}$ and chromaticity coordinates (x, y) of the LED at steady state are described in (6)–(8), shown at the bottom of this page

It can be seen from (7) and (8) that the chromaticity coordinates (x, y) approach the values corresponding to I_H and I_L at large and small duty cycles, respectively, but mix nonlinearly at intermediate duty cycles. To account for this nonlinear color-mixing behavior, one needs to resolve to the use of numerical calculations for an exact description of the color-shift properties under bilevel dimming, while an analytical formulation of the model is desired to provide direct insights on the physical parameters that affect the color-shift properties. Since the latter is the objective of this study, approximations to (7) and (8) should be sought in order to facilitate a further development of the model in a more useful analytical form.

Fig. 4 shows the measured chromaticity coordinate (x, y) under various I_L values with $I_H = 1000\,\mathrm{mA}$. The dashed lines represent the linear approximations to the measured trends by duty-cycle averaging of the coordinate values at I_H and I_L, as given by (9) and (10). It is clear from the figures that the errors produced by the linear approximations are significant when I_H is significantly higher than I_L, but, as expected, the discrepancies decrease as the difference between I_H and I_L is narrowed. If one can constrain the relative magnitude between I_H and I_L to within a reasonable size as governed by individual

$$\overline{I_f} = D \cdot I_H + (1 - D) \cdot I_L \tag{6}$$

$$x = \frac{D \cdot X\left(I_H, T_j\right) + (1 - D) \cdot X\left(I_L, T_j\right)}{D \cdot \left[X\left(I_H, T_j\right) + Y\left(I_H, T_j\right) + Z\left(I_H, T_j\right)\right] + (1 - D) \cdot \left[X\left(I_L, T_j\right) + Y\left(I_L, T_j\right) + Z\left(I_L, T_j\right)\right]} \tag{7}$$

$$y = \frac{D \cdot Y\left(I_H, T_j\right) + (1 - D) \cdot Y\left(I_L, T_j\right)}{D \cdot \left[X\left(I_H, T_j\right) + Y\left(I_H, T_j\right) + Z\left(I_H, T_j\right)\right] + (1 - D) \cdot \left[X\left(I_L, T_j\right) + Y\left(I_L, T_j\right) + Z\left(I_L, T_j\right)\right]}. \tag{8}$$

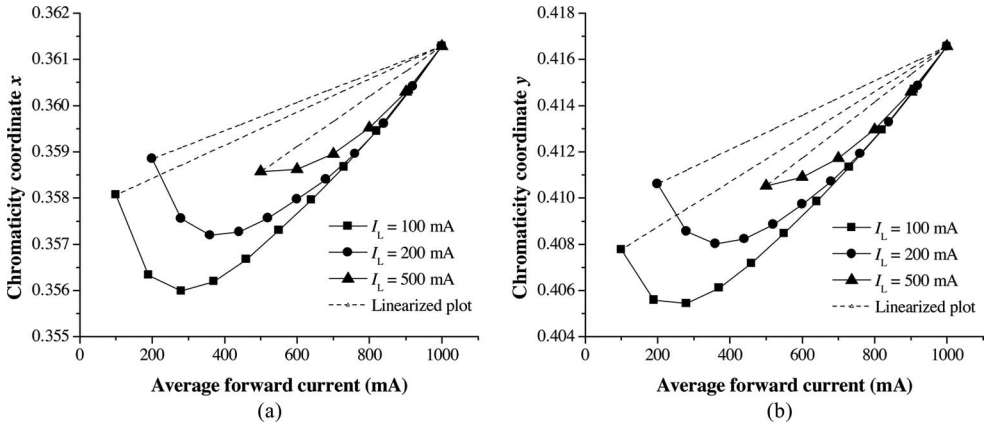

Fig. 4. Measured chromaticity coordinates [(a) x, (b) y] under various I_L values. I_H is fixed at 1000 mA for all cases. Dashed lines represent the chromaticity coordinates (x, y) computed by linear averaging of the coordinate values at I_H and I_L by the duty cycle.

types/brands of white LEDs, the simplified model to be derived in the following steps will serve the purpose of generating a qualitative view of the impacts of forward current level and junction temperature on their color-shift properties, and become the basis for a further development in Section IV. Therefore, noting the constraint described earlier, (7) and (8) are substituted with (9) and (10) in the subsequent derivation:

$$x = D \cdot x\left(I_H, T_j\right) + (1 - D) \cdot x\left(I_L, T_j\right) \tag{9}$$

$$y = D \cdot y\left(I_H, T_j\right) + (1 - D) \cdot y\left(I_L, T_j\right). \tag{10}$$

Since both I_H and I_L are fixed in amplitude, (7) and (8) can be rewritten as

$$x = D \cdot x_H\left(T_j\right) + (1 - D) \cdot x_L\left(T_j\right) \tag{11}$$

$$y = D \cdot y_H\left(T_j\right) + (1 - D) \cdot y_L\left(T_j\right) \tag{12}$$

which simplify (x, y) to functions of the duty cycle D and LED's junction temperature T_j only. When both D and T_j undergo small changes, the corresponding change in x (and similarly for y) is given by

$$\begin{aligned} \mathrm{d}x &= (x_H - x_L) \cdot \mathrm{d}D + D \cdot \mathrm{d}x_H + (1 - D) \cdot \mathrm{d}x_L \\ &= (x_H - x_L) \cdot \mathrm{d}D + D \cdot (\mathrm{d}x_H - \mathrm{d}x_L) + \mathrm{d}x_L \end{aligned} \tag{13}$$

where

$$\mathrm{d}x_{(\mathrm{H,L})} = \frac{\partial x_{(\mathrm{H,L})}}{\partial T_j} \cdot \mathrm{d}T_{j.} \tag{14}$$

Substituting (14) into (13) gives

$$\begin{aligned} \mathrm{d}x = (x_H - x_L) \cdot \mathrm{d}D + D \cdot \left(\frac{\partial x_H}{\partial T_j} - \frac{\partial x_L}{\partial T_j}\right) \cdot \mathrm{d}T_j \\ + \frac{\partial x_L}{\partial T_j} \cdot \mathrm{d}T_{j.} \end{aligned} \tag{15}$$

From Fig. 3, it can be seen that, to a very good approximation, both x and y are linear functions of T_j and the lines for different current amplitudes are nearly parallel to each other. Therefore, the following assumption is made:

$$\frac{\partial\left(x, y\right)_H}{\partial T_j} \approx \frac{\partial\left(x, y\right)_L}{\partial T_j} = \frac{\partial\left(x, y\right)}{\partial T_j}. \tag{16}$$

By using this assumption and making the substitutions $\Delta x = (x_H - x_L)$ and $\Delta y = (y_H - y_L)$, one obtains the following simplified equations for $\mathrm{d}x$ and $\mathrm{d}y$:

$$\begin{aligned} \mathrm{d}x &= \Delta x \cdot \mathrm{d}D + \frac{\partial x}{\partial T_j} \cdot \mathrm{d}T_j \\ \mathrm{d}y &= \Delta y \cdot \mathrm{d}D + \frac{\partial y}{\partial T_j} \cdot \mathrm{d}T_j. \end{aligned} \tag{17}$$

In general, the color shift of a light source is measured by the geometrical distance ϵ of a color point (x, y) from a predetermined reference, as given by

$$\mathrm{d}\epsilon = \sqrt{(\mathrm{d}x)^2 + (\mathrm{d}y)^2}. \tag{18}$$

Substituting (17) into (18) gives

$$\mathrm{d}\epsilon = \sqrt{\lambda_1 \cdot (\mathrm{d}D)^2 + \lambda_2 \cdot (\mathrm{d}D) \cdot (\mathrm{d}T_j) + \lambda_3 \cdot (\mathrm{d}T_j)^2} \tag{19}$$

where

$$\lambda_1 = (\Delta x)^2 + (\Delta y)^2 \tag{20}$$

$$\lambda_2 = 2\left(\Delta x \cdot \frac{\partial x}{\partial T_j} + \Delta y \cdot \frac{\partial y}{\partial T_j}\right) \tag{21}$$

$$\lambda_3 = \left(\frac{\partial x}{\partial T_j}\right)^2 + \left(\frac{\partial y}{\partial T_j}\right)^2. \tag{22}$$

Further simplifications can be made to (19) by recognizing the in-phase relationship between x and y (as verified by Figs. 2 and 3). They represent the degree of stimulation of the red and green cones of human eyes, respectively, both of which originate from the blue-induced phosphor emission from the white LED. Hence, two constants α and β can be introduced and substituted into (20)–(22):

$$\alpha = \frac{\Delta y}{\Delta x} \tag{23}$$

$$\beta = \frac{\partial y/\partial T_j}{\partial x/\partial T_j} \tag{24}$$

$$\lambda_1 = \left(1+\alpha^2\right)\cdot(\Delta x)^2 \tag{25}$$

$$\lambda_2 = 2\left(1+\alpha\beta\right)\cdot\Delta x\cdot\frac{\partial x}{\partial T_j} \tag{26}$$

$$\lambda_3 = \left(1+\beta^2\right)\cdot\left(\frac{\partial x}{\partial T_j}\right)^2. \tag{27}$$

For an LED mounted on a fixed heat sink, T_j is determined by the the total heat dissipated and the total junction-to-ambient thermal resistance $R_{j\text{-}a}$, as given by (28), where $k_{(H,L)}$ represents the portion of input electrical power $V_{(H,L)}\cdot I_{(H,L)}$ is dissipated as heat.

$$\begin{aligned} T_j &= R_{j\text{-}a}\cdot\left[D\cdot k_H\cdot V_H\cdot I_H+(1-D)\cdot k_L\cdot V_L\cdot I_L\right]+T_a \\ &= R_{j\text{-}a}\cdot\left[D\cdot\left(k_H\cdot V_H\cdot I_H-k_L\cdot V_L\cdot I_L\right)+k_L\cdot V_L\cdot I_L\right] \\ &\quad +T_a. \end{aligned} \tag{28}$$

Since the total heat dissipated is related to the average electrical power delivered to the LED, hence the duty cycle, by intuition (19) can be reformulated as a single-variable function in D *if the* ambient temperature T_a is constant over the course of dimming, i.e. $\mathrm{d}T_a = 0$. Differentiating T_j with respect to D gives

$$\begin{aligned} \mathrm{d}T_j &= R_{j\text{-}a}\cdot\left(k_H\cdot V_H\cdot I_H-k_L\cdot V_L\cdot I_L\right)\cdot\mathrm{d}D \\ &= \Omega\cdot\mathrm{d}D. \end{aligned} \tag{29}$$

By substituting (29) into (19), the functional dependence of ϵ on D is obtained. Integrating (30) shows a linear relationship between ϵ and D as $f(\Omega)$ is constant and depends on $R_{j\text{-}a}$ and the difference in current levels $\Delta I = (I_H - I_L)$ only:

$$\begin{aligned} \mathrm{d}\epsilon &= \left(\sqrt{\lambda_1+\lambda_2\cdot\Omega+\lambda_3\cdot\Omega^2}\right)\cdot\mathrm{d}D \\ &= f(\Omega)\cdot\mathrm{d}D. \end{aligned} \tag{30}$$

It should be noted that the simplified model does not include the following effects. First, the junction-to-case thermal resistance $R_{j\text{-}c}$ of LED, which constitutes $R_{j\text{-}a}$, is not constant but depends on several factors such as the heat sink's thermal resistance and orientation, LED size and mounting structure, and the ambient temperature [15]. These collective effects, however, are difficult to be modeled mathematically. Second, experimental data show that, to a good approximation, the forward voltage of LED varies inverse proportionally with T_j [17], Since the simplified color-shift model is only aimed at providing the required insights to the discussion on color-shift reduction methods in Section IV, such complexities are avoided in the derivation.

IV. Color-Shift Reduction Methods Based on Bilevel Drive

For the comfort of human vision under illumination, the color point of a light source must not vary significantly over the course of dimming. For example, the color variations of fluorescent lamps on the CIE 1960 uniform chromaticity diagram are usually specified to within $\Delta(uv) = 0.003$ to ensure that the color difference is not noticeable by average human eyes [18]. For high-end applications such as LCD backlighting, an even more stringent requirement of $\Delta(uv) = 0.002$ is demanded [19], [20]. Although these limits are commonly specified in CIE 1960 (u, v), the older coordinates CIE 1931 (x, y) were used in Section III to enable a simplification of the model by adopting the linear $\partial(x,y)/\partial I_f$ and $\partial(x,y)/\partial T_j$ characteristics, which is not available with (u, v). In practice, $\Delta(uv)$ cannot be transformed directly from $\Delta(xy)$ but it must be computed stepwise through the following mapping equations, where (u_0, v_0) denotes the reference color point:

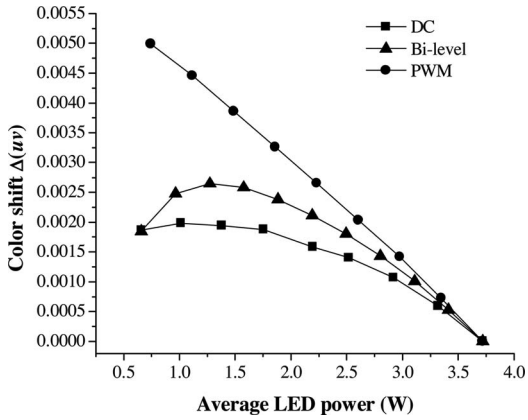

Fig. 5. Measured color shift $\Delta(uv)$ of a white-LED sample (LUXEON K2) driven by three types of current waveforms [dc, PWM (0, 1000 mA), and bilevel (200, 1000 mA)]. The sample is mounted on a heat sink with thermal resistance $R_{\mathrm{hs}\text{-}a} = 13.4°\mathrm{C/W}$.

$$u = \frac{4x}{-2x+12y+3} \tag{31}$$

$$v = \frac{6y}{-2x+12y+3} \tag{32}$$

$$\Delta(uv) = \sqrt{(u-u_0)^2+(v-v_0)^2}. \tag{33}$$

Fig. 5 shows the measured color shifts of the LUXEON K2 white-LED sample under dc, PWM, and bilevel driving/dimming. For the PWM case, the peak current is fixed at $1000\ \mathrm{mA}$, and for the bilevel case, I_H and I_L are fixed at $1000\ \mathrm{mA}$ and $200\ \mathrm{mA}$, respectively. It can be seen that the limit of $\Delta(uv) = 0.002$ can be easily exceeded when the LED is driven/dimmed by PWM. The situation is improved when bilevel current is used, although the limit is still exceeded over part of the dimming range. The best color stability is achieved when the LED is driven/dimmed by dc current, but, as discussed before, this leads to a nonlinear dimming profile due to the saturable luminous output characteristic of LEDs. On the other hand, the advantage of linear dimming by PWM is largely offset by the disadvantages of poor color stability and low luminous output. It can be shown that, with suitably selected operating parameters, an LED driven by bilevel current has a surpassing color-stability performance compared to PWM while maintaining a linear dimming profile and delivering higher luminous output.

In accordance to (29) and (30), the degree of color shift of an LED driven/dimmed by bilevel current is affected by the parameter Ω, which in turn is a function of the junction-to-ambient thermal resistance $R_{j\text{-}a}$ and the difference in current levels $\Delta I = (I_H - I_L)$. One can deduce that $f(\Omega)$ should be decreased as much as possible in order to minimize the overall color shift of an LED over dimming. In practice, this must be realized by appropriate selections of $R_{j\text{-}a}$ and ΔI. Based on these implications, two color-shift reduction methods can be proposed, as will be discussed next.

A. Stationary Method

This method focuses on the selection of $R_{j\text{-}a}$ that minimizes the overall color shift ϵ over dimming. One can understand the validity of this method by considering the two aspects of peak-emission-wavelength shift of an LED under bilevel drive. In general, an increase in current amplitude and junction temperature leads to a more significant blue-shift and red-shift in the peak emission wavelength, respectively [14]. On the first aspect, as the LED is dimmed by decreasing the duty cycle from $D = 1$ to $D = 0$, the degree of blue-shift is gradually reduced as the contribution of I_H decreases and I_L becomes increasingly dominant. This continues until a minimum blue-shift is attained at $D = 0$ and $\overline{I_f} = I_L$. On the second aspect, dimming the LED from $D = 1$ to $D = 0$ leads to a decrease in junction temperature, which is accompanied by a reduction in the degree of red-shift until a minimum red-shift is attained at $D = 0$ and $\overline{I_f} = I_L$. Since the wavelength shifts due to current amplitude and junction temperature change constantly act in opposite directions and compensate each other, as verified by the measured data in Figs. 2 and 3, it is intuitively valid to propose a method for controlling the rate of junction temperature change to ensure that it induces a certain degree of red-shift that "correctly" balances the degree of blue-shift induced by a given change in current amplitude. This can be achieved by means of selection of $R_{j\text{-}a}$.

According to (30), solving $f'(\Omega) = 0$ gives the value of Ω that minimizes $\mathrm{d}\epsilon$ (since $\lambda_3 > 0$), as follows:

$$f'(\Omega) = 0 \Rightarrow \Omega|_{\min f} = -\frac{\lambda_2}{2\lambda 3} = -\left(\frac{1+\alpha\beta}{1+\beta^2}\right)\cdot\left(\frac{\Delta x}{\partial x/\partial T_j}\right) \tag{34}$$

$$\mathrm{d}\epsilon|_{\min} = \left(\sqrt{\frac{(\alpha-\beta)^2\cdot(\Delta x)^2}{1+\beta^2}}\right)\cdot \mathrm{d}D. \tag{35}$$

It is implied in (34) that when the difference in current levels $\Delta I = (I_H - I_L)$ is decreased, and results in a smaller Δx, a smaller $\Omega|_{\min f}$ should be chosen so that the red-shift due to junction temperature change does not overcompensate the reduced blue-shift due to a smaller ΔI. Finally, from (29)

$$R_{j\text{-}a}|_{\min f} = (R_{j\text{-}c} + R_{\mathrm{hs}\text{-}a})|_{\min f} = \frac{\Omega|_{\min f}}{k_H\cdot V_H\cdot I_H - k_L\cdot V_L\cdot I_L}. \tag{36}$$

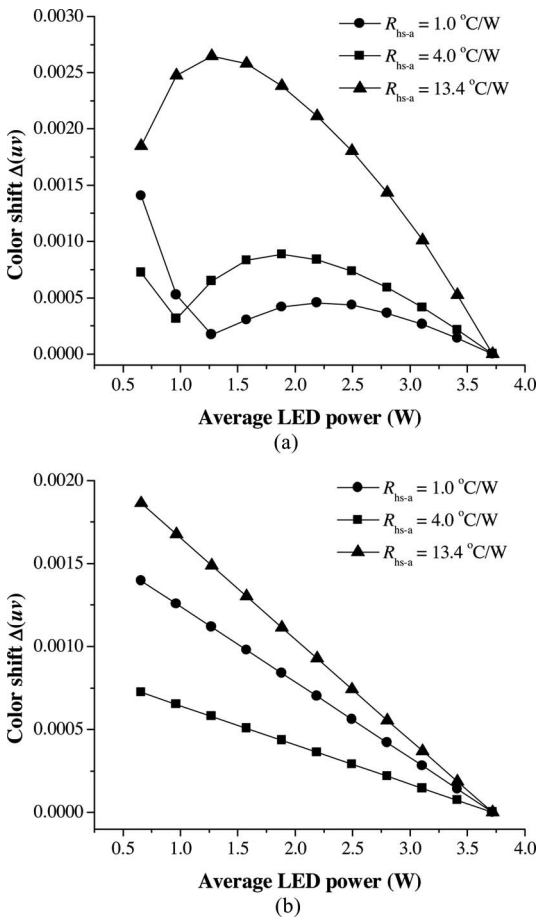

Fig. 6. (a) Measured and (b) calculated color shift $\Delta(uv)$ of a white-LED sample (LUXEON K2) mounted on different heat sinks with the chromaticity coordinates (u, v) at $\overline{I_f} = 1000$ mA as reference.

Therefore, for a given choice of (I_L, I_H), the required total junction-to-ambient thermal resistance can be obtained from (36), from which the required heat sink's thermal resistance $R_{\mathrm{hs}\text{-}a}$ can be estimated if the junction-to-case thermal resistance $R_{j\text{-}c}$ of the LED is known (from datasheet). It should be noted that (36) is not meant to be used for exact calculations as it has not included the various nonlinear effects discussed earlier. However, it should provide the insights on how the heat sink's thermal resistance should be chosen for a given $\Delta I = (I_H - I_L)$ for color-shift minimization. In practice, to achieve this objective, some fine-tuning will be required to account for these nonlinear effects. Once the required heat sink's thermal resistance has been identified, it requires no further adjustment until a new (I_L, I_H) is defined; therefore, this method is *stationary* by nature.

For an illustration of this method, the color shift $\Delta(uv)$ of a white-LED sample (LUXEON K2) mounted on different heat sinks was measured under different drive conditions. The measured data are shown in Fig. 6(a), and the calculated values are shown in Fig. 6(b) for comparisons. For the calculations, I_H and I_L are fixed at 1000 mA and 200mA, respectively, and the corresponding diode voltages are obtained from the manufacturer's datasheet as $V_H = 3.7$ V and $V_L = 3.3$ V. The

thermal dissipation factors, k_H and k_L, of LUXEON K2 are taken as 0.85 from [21]. Other color-shift parameters, including $\Delta x = -4.56 \times 10^{-3}$, $\partial x/\partial T_j = 1.20 \times 10^{-4\circ}\mathrm{C}^{-1}$, $\alpha = 1.69$, and $\beta = 1.96$, are estimated from the experimental data shown in Figs. 2 and 3. Substituting these values into (36) gives the "optimum" heat sink's thermal resistance value as

$$R_{\text{hs-}a}|_{\min f} \approx 4.0^{\circ}\text{C/W}. \tag{37}$$

It can be seen from Fig. 6(b) that the theoretical "optimum" thermal resistance value does produce the smallest predicted color shift among the three thermal resistance values considered. However, since the model considers only the initial and final chromaticity coordinate values and assumes a linear interpolation between them for the computation of the intermediate coordinate values, it fails to predict the nonlinear behavior of the color-shift trajectory over the course of dimming. From this perspective, the mathematical model can be conceptualized as an approximation that produces an *average* color-shift representation of the actual trajectory, which, understandably, is a natural consequence of the linear approximations adopted in (9) and (10). More accurate approximations to (7) and (8) are needed to resolve the disagreement between experimental measurements and model calculations.

In Fig. 6(a), it is interesting to observe the local minimum points that exist in the measured color shifts for $R_{\text{hs-}a} = 1.0^{\circ}$C/W and $R_{\text{hs-}a} = 4.0^{\circ}$C/W. As the LED is dimmed from 1000 mA, the change in duty cycle alters the mixing ratio between the color contributions from I_H and I_L and leads to a color shift, which is partially compensated by the opposing effect imposed by a corresponding change in junction temperature. The local minimum points represent the conditions under which these two opposing effects have attained the optimum balance. The balance is upset when the LED's operation departs from these conditions. It should be noted that the color stabilization mechanism by the opposing effects of forward current level and junction temperature is not existent for PWM dimming, as it has current levels $(0, I_H)$ that are fixed over the course of dimming; hence, the color shift due to junction temperature change is left uncompensated in the absence of an opposite shift due to current amplitude change. The impacts of AM and PWM dimming on the color shift of white LEDs are discussed in [22] and [23] based on experimental measurements. However, the effects of current amplitude (or duty cycle) and junction temperature were not carefully distinguished in these studies. These issues are addressed in our recent work [5]. For a more generalized approach to driving/dimming white LEDs, it is advantageous to operate them with two dimming control parameters, i.e., duty cycle and current levels [10], [11], for an improved color-stability performance.

B. Adaptive Method

In general, the stationary method should be adopted when the choice of thermal resistance value is not restricted. This is, however, not possible in many practical applications because the available choices are often limited by the volume, weight, geometry, orientation, and even cost constraints being imposed on the lighting system. Under these constraints, the thermal resistance value closest to the one predicted by (36) should be chosen, while, according to (29) and (30), a further color-shift reduction can be accomplished dynamically by an adaptive change of $\Delta I = (I_H - I_L)$ with duty cycle over dimming. The concept can be explained by the illustrative example shown in Fig. 7.

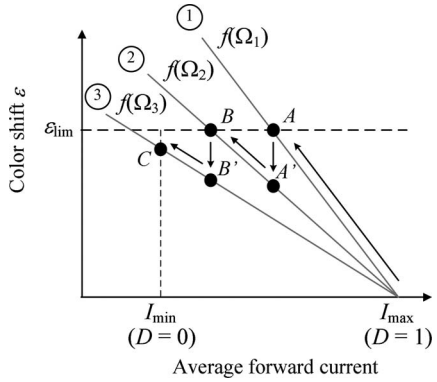

Fig. 7. Graphical illustration of the color-shift reduction method based on adaptive change of $\Delta I = (I_H - I_L)$ with duty cycle (or average forward current).

Assume that an LED is dimmed from $D = 1$ with an initial Ω $(= \Omega_1)$, which is defined by the initial current-level difference $(\Delta I)_1$ and a heat sink's thermal resistance $R_{\text{hs-}a}$ that causes the color shift of the LED to increase beyond the allowable limit $\epsilon_{\lim}$ over part of the dimming range. By using the color point at $\overline{I_f} = I_{\max}$ as reference, the color shift of the LED will increase along line 1 as D is decreased, until the limit $\epsilon_{\lim}$ is reached at A. To prevent the color shift from increasing further, a new Ω $(= \Omega_2)$ can be defined such that the dimming path will continue from A' on line 2, which gives rise to a reduced color shift located away from the limit. Technically, since $R_{\text{hs-}a}$ is constant, this can only be achieved by selecting a new current-level difference $(\Delta I)_2$. The selection of $(\Delta I)_2$ is, nevertheless, not arbitrary. To ensure a smooth transition from line 1 to line 2, the same average forward current must be maintained while ΔI is varied from $(\Delta I)_1$ to $(\Delta I)_2$, implying that I_H and I_L must be adjusted concurrently as governed by $I_L = \left(\overline{I_f} - D \cdot I_H\right) / (1 - D)$. A closer look at the functional form of $f(\Omega)$ suggests that ΔI can be either increased or decreased during this step since there are two approaches by which the color shift can be reduced, as shown by Fig. 8, depending on the location of the initial operating point. Physically, this means that the initial mismatch between the selected heat sink's thermal resistance and current levels could result in an under- or overcompensation between the color shifts induced by current amplitude and junction temperature changes. The nature of this mismatch will determine the initial point in the color-shift trajectory.

With the new current-level difference $(\Delta I)_2$, the color shift will now increase along line 2 as D is further decreased, until the limit $\epsilon_{\lim}$ is reached at B. At this point, a new ΔI, $(\Delta I)_3$, is required and can be selected in the same manner as before. This procedure should be repeated until the minimum duty

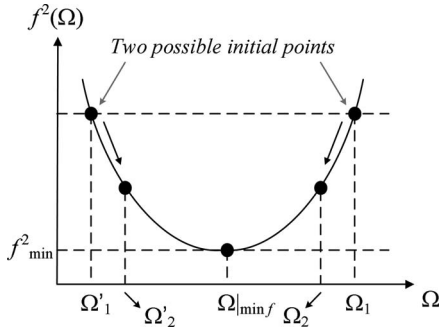

Fig. 8. Graphical illustration of the two possible initial conditions (Ω_1 and Ω'_1) for approaching the point of minimum color shift $\left(\Omega|_{\min f}, f^2_{\min}\right)$.

TABLE I
OPERATING PARAMETERS FOR THE ADAPTIVE BIL

D	$\overline{I_f}$ (mA)	$\overline{P_{\rm LED}}$ (W)	$I_{\rm H}$ (mA)	$I_{\rm L}$ (mA)	ΔI (mA)	$\Delta\,(uv)$
0.0	200	0.66	200	200	0	0.001864
0.1	280	0.94	280	280	0	0.001958
0.2	360	1.23	360	360	0	0.001958
0.3	440	1.53	440	440	0	0.001916
0.4	520	1.84	600	470	130	0.001899
0.5	600	2.15	800	400	400	0.001828
0.6	680	2.50	1000	200	800	0.001805
0.7	760	2.80	1000	200	800	0.001434
0.8	840	3.11	1000	200	800	0.001012
0.9	920	3.41	1000	200	800	0.000525
1.0	1000	3.72	1000	200	800	0.000000

cycle ($D = 0$) or average forward current ($\overline{I_f} = I_L$) is reached. As a result of these steps, the overall color shift of the LED is constantly restricted below the limit by varying ΔI dynamically over the course of dimming. In practice, to realize this method, the instances of A and B can be found by initial calibration and the corresponding ΔI's are programmed into the dimming controller circuitries of LED drivers. In comparison to the stationary method, this method is considered *adaptive* by nature.

The LED driver shown in Fig. 9 is used to verify the proposed method. It is based on buck topology with an adjustable reference current. In this experiment, the LED is dimmed from $D = 1$ in steps of $\Delta D = 0.1$, with the reference current initially set to pulsate between $I_H = 1000\ \mathrm{mA}$ and $I_L = 200\ \mathrm{mA}$ at 400 Hz. By using the color point at $\overline{I_f} = 1000\ \mathrm{mA}$ as reference, the chromaticity coordinates of the emitted light are monitored by a fibre-optic spectrometer, USB4000 produced by Ocean Optics, and the color shift $\Delta\,(uv)$ are calculated for each measurement point to check if the limit $\Delta\,(uv) = 0.002$ is exceeded. When the color shift increases beyond this limit, I_H and I_L are adjusted concurrently while keeping the average forward current unchanged, and the new color shift is calculated and checked against the limit. These steps are iterated until the color shift resides below the limit. When this condition is satisfied, the LED is further dimmed by decreasing the duty cycle until the limit is again exceeded, during which a search for new I_H and I_L is initiated and performed in the same manner as aforementioned. These steps are repeated until $D = 0$ is reached.

Fig. 10 shows the color shift measured with and without using the proposed adaptive method. When the adaptive method is not used, I_H and I_L are fixed at $1000\ \mathrm{mA}$ and $200\ \mathrm{mA}$, respectively,

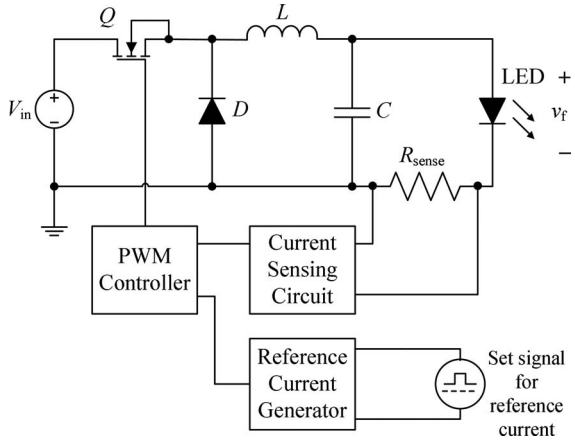

Fig. 9. Buck-based LED driver with an adjustable reference current to be used for verifying the proposed adaptive color-shift reduction method.

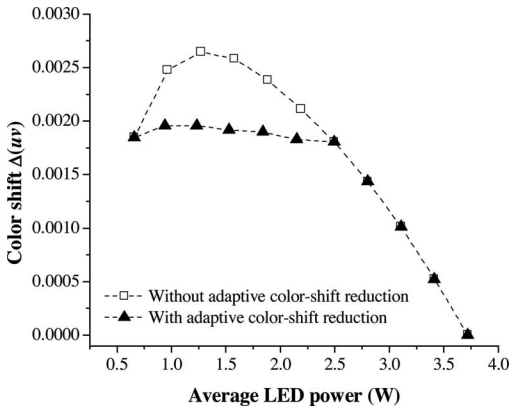

Fig. 10. Measured color shift $\Delta\,(uv)$ of a white-LED sample (LUXEON K2) dimmed with and without using the adaptive color-shift reduction method.

over the entire dimming range, where the color shift is observed to increase beyond the limit $\Delta\,(uv) = 0.002$ for $D \leq 0.5$. To keep the color shift below the limit, ΔI is narrowed to $400\ \mathrm{mA}$ at $D = 0.5$ and $130\ \mathrm{mA}$ at $D = 0.4$. For $D \leq 0.3$, ΔI is reduced to zero; hence, dimming is achieved by AM in this region. Therefore, it is shown that, with a given thermal design, a further reduction in the overall color shift over dimming is possible by adaptively adjusting the combination of current levels and duty cycle. However, the improved color stability is achieved at the drawbacks of added complexity of the control circuitry and the necessity for calibration in order to identify the required values of ΔI under various duty cycles or dimming conditions. For implementation, a digital signal processor (DSP) is typically required for storing the LED's chromaticity information and computing the required forward current levels I_H and I_L based on the sensed LED's voltage, current, and case temperature.

V. CONCLUSION

The color-shift properties of phosphor-based white LEDs under bilevel drive were discussed using a simplified mathematical color-shift model developed in this study. It was shown that

the color-stability performance of a bilevel-driven LED over dimming is a result of the complex interactions between the selected current levels, duty cycle, and junction temperature (hence thermal design). In the model, these complex interactions were conveniently summarized in a single function $f(\Omega)$ that is subject to minimization for an optimum color stability. The dependences of Ω on the heat sink's thermal resistance and the difference in current levels indicate the two possible approaches for color-shift reduction over dimming. For some preselected current levels, a heat sink's thermal resistance that minimizes the overall color shift can be uniquely identified. Since this method gives rise to a global minimum color shift, it should be adopted whenever possible. When the choices of heat sink's thermal resistance and current levels are restricted, a reduction in color shift is still possible by adaptively adjusting the combination of current levels and duty cycle over dimming. The theoretical details of both methods were presented and discussed in detail, and their validity was verified by experimental measurements. The availability of 2-D control of luminosity and color stability with bilevel drive renders it an attractive driving/dimming method that encompasses the all-round benefits of linear dimming, improved color stability, and higher luminous output.

Although the issue of phosphor's aging is not explicitly considered in this study, it is believed that, since the wavelength shift due to forward current level and junction temperature changes is a physical and well documented phenomenon, the cancellation between the blue-shift and red-shift effects on the dominant wavelength ($\approx$460 nm), which is the key factor leading to color stabilization, is operative under all phosphor's aging conditions. Therefore, when the dominant wavelength's shift is minimized by the proposed methods, the phosphor, aged or nonaged, will be excited by the same stabilized dominant wavelength at all time. Despite that different colors may be emitted by aged and nonaged phosphor when excited by the same dominant wavelength, the degree of color shift over dimming under a given phosphor's aging condition will remain governed by the methods reported in this study. This proposition will be verified in a future work.

REFERENCES

[1] J. R. Coaton and A. M. Marsden, *Lamps and Lighting*, 4th ed. London, U.K.: Butterworth-Heinemann, 2001.

[2] Y. K. E. Ho, S. T. S. Lee, H. S. H. Chung, and S. Y. Hui, "A comparative study on dimming control methods for electronic ballasts," *IEEE Trans. Power Electron.*, vol. 16, no. 6, pp. 828–836, Nov. 2001.

[3] H. S. H. Chung, N. M. Ho, W. Yan, P. W. Tam, and S. Y. Hui, "Comparison of dimmable electromagnetic and electronic ballast systems—An assessment on energy efficiency and lifetime," *IEEE Trans. Ind. Electron.*, vol. 54, no. 6, pp. 3145–3154, Dec. 2007.

[4] J. Ribas, J. M. Alonso, E. L. Corominas, A. J. Calleja, and M. Rico-Secades, "Design considerations for optimum ignition and dimming of fluorescent lamps using a resonant inverter operating open loop," in *Proc. IEEE 38th IAS Annu. Meeting* Ind. Appl. Conf., Oct. 12–15, 1998, vol. 3, pp. 2068–2075.

[5] K. H. Loo, Y. M. Lai, S. C. Tan, and Chi K. Tse, "On the color stability of phosphor-converted white LEDs under DC, PWM, and bilevel drive," *IEEE Trans. Power Electron.*, to be published.

[6] S. D. Lester, M. J. Ludowise, K. P. Killeenm, B. H. Perez, J. N. Miller, and S. J. Rosner, "High-efficiency InGaN MQW blue and green LEDs," *J. Crystal Growth*, vol. 189/190, pp. 786–789, Jun. 1998.

[7] V. Adivarahan, A. Chitnis, J. P. Zhang, M. Shatalov, J. W. Wang, G. Simin, and M. Asif, "Ultraviolet light-emitting diodes at 340 nm using quaternary AlInGaN multiple quantum wells," *Appl. Phys. Lett.*, vol. 79, no. 25, pp. 4240–4242, Dec. 2001.

[8] T. Mukai, M. Yamada, and S. Nakamura, "Characteristics of InGaN-based UV/blue/green/amber/red light-emitting diodes," *Jpn. J. Appl. Phys. Part 1*, vol. 38, no. 7A, pp. 3976–3981, Jul. 1999.

[9] S. Nakamura, T. Mukai, and M. Senoh, "Candela-class high-brightness InGaN/AlGaN double-heterostructure blue-light-emitting diodes," *Appl. Phys. Lett.*, vol. 64, no. 13, pp. 1687–1689, Mar. 1994.

[10] W. K. Lun, K. H. Loo, S. C. Tan, Y. M. Lai, and Chi K. Tse, "Bilevel current driving technique for LEDs," *IEEE Trans. Power Electron.*, vol. 24, no. 12, pp. 2920–2932, Dec. 2009.

[11] K. H. Loo, W. K. Lun, S. C. Tan, Y. M. Lai, and C. K. Tse, "On driving techniques for LEDs: Toward a generalized methodology," *IEEE Trans. Power Electron.*, vol. 24, no. 12, pp. 2967–2976, Dec. 2009.

[12] S. Nakamura, "InGaN/AlGaN blue-light-emitting diodes," *J. Vacuum Sci. Technol. A*, vol. 13, no. 3, pp. 705–710, May/Jun. 1995.

[13] T. Mukai, M. Yamada, and S. Nakamura, "Current and temperature dependences of electroluminescence of InGaN-based UV/Blue/Green light-emitting diodes," *Jpn. J. Appl. Phys. Part 2*, vol. 37, no. 11B, pp. L1358–L1361, Dec. 1998.

[14] R. Mueller-Mach, G. O. Mueller, M. R. Krames, and T. Trottier, "High-power phosphor-converted light-emitting diodes based on III-nitrides," *IEEE J. Sel. Topics Quantum Electron.*, vol. 8, no. 2, pp. 339–345, Mar./Apr. 2002.

[15] S. Y. (Ron) Hui, and Y. X. Qin, "A general photo-electro-thermal theory for light emitting diode (LED) systems," *IEEE Trans. Power Electron.*, vol. 24, no. 8, pp. 1967–1976, Aug. 2009.

[16] *LUXEON K2*, Technical datasheet DS51, Philips Lumileds, 2008.

[17] S. Chhajed, Y. Xi, Y.-L. Li, Th. Gessmann, and E. F. Schubert, "Influence of junction temperature on chromaticity and color-rendering properties of trichromatic white-light sources based on light-emitting diodes," *J. Appl. Phys.*, vol. 97, no. 5, pp. 054506-1–054506-8, Mar. 2005.

[18] S. Muthu, F. J. Schuurmans, and M. D. Pashley, "Red, Green, and Blue LEDs for white light illumination," *IEEE J. Sel. Topics Quantum Electron.*, vol. 8, no. 2, pp. 333–338, Mar./Apr. 2002.

[19] S. Muthu, F. J. Schuurmans, and M. D. Pashley, "Red, Green, and Blue LED based white light generation: Issues and control," in *Proc. 37th IAS Annu. Meeting Conf. Rec. Ind. Appl.*, Oct.13–18, 2002, vol. 1, pp. 327–333.

[20] X. Qu, S. C. Wong, and C. K. Tse, "Temperature measurement technique for stabilizing the light output of RGB LED lamps," *IEEE Trans. Instrum. Meas.*, vol. 59, no. 3, pp. 661–670, Mar. 2010.

[21] Y. Qin, D. Lin, and S. Y. (Ron) Hui, "A simple method for comparative study on the thermal performance of LEDs and fluorescent lamps," *IEEE Trans. Power Electron.*, vol. 24, no. 7, pp. 1811–1818, Jul. 2009.

[22] M. Dyble, N. Narendran, A. Bierman, and T. Klein, "Impact of dimming white LEDs: Chromaticity shifts due to different dimming methods," *Proc. SPIE*, vol. 5941 pp. 291–299, 2005.

[23] Y. Gu, N. Narendran, T. Dong, and H. Wu, "Spectral and luminous efficacy change of high-power LEDs under different dimming methods," *Proc. SPIE*, vol. 6337, pp. 63370J-1–63370J-8, 2006.

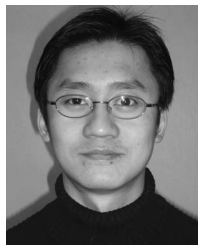

K. H. Loo (S'97–M'99) received the B.Eng. (Hons.) degree in electronic engineering and the Ph.D. degree in from the University of Sheffield, Sheffield, U.K., in 1999 and 2002, respectively.

From November 2002 to November 2004, he was a Postdoctoral Fellow with the Japan Society for the Promotion of Science (JSPS) during which he carried out researches on the mercury-free fluorescent lamp diagnostics and modeling in Ehime University, Shikoku, Japan. From March 2005 to August 2006, he was an Electronic Engineer in a local lighting company in Hong Kong. He joined The Hong Kong Polytechnic University, Kowloon, Hong Kong, in August 2006, where he is currently an Instructor at the Faculty of Engineering. His research interests include LED lighting and control circuitry designs, diagnostics, and modeling of fuel cells for portable applications.

Y. M. Lai (M'92) received the B.Eng. degree in electrical engineering from the University of Western Australia, Perth, Australia, in 1983, the M.Eng.Sc. degree in electrical engineering from University of Sydney, Sydney, Australia, in 1986, and the Ph.D. degree from Brunel University, London, U.K., in 1997.

He is currently an Associate Professor with The Hong Kong Polytechnic University, Kowloon, Hong Kong. His research interests include computer-aided design of power electronics and nonlinear dynamics.

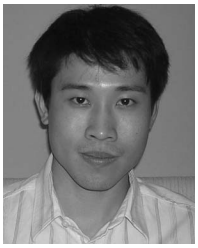

Siew-Chong Tan (S'00–M'06) received the B.Eng. (Hons.) and M.Eng. degrees in electrical and computer engineering from the National University of Singapore, Singapore, in 2000 and 2002, respectively, and the Ph.D. degree from The Hong Kong Polytechnic University, Kowloon, Hong Kong, in 2005.

From October 2005 to February 2009, he was a Research Associate, a Postdoctoral Fellow, and then as a Lecturer in the Department of Electronic and Information Engineering, The Hong Kong Polytechnic University, where he is currently an Assistant Professor. His current research interests include nonlinear control of power converters, switched-capacitor converter circuits and control, and on developing power-electronic based circuits for light-emitting diodes and fuel cells.

Chi K. Tse (M'90–SM'97–F'06) received the B.Eng. (first class Hons.) degree in electrical engineering and the Ph.D. degree from the University of Melbourne, Melbourne, Vic., Australia, in 1987 and 1991, respectively.

He is currently the Chair Professor and the Head of the Department of Electronic and Information Engineering, The Hong Kong Polytechnic University, Kowloon, Hong Kong. His research interests include power electronics, complex networks, and nonlinear systems. He is the author of *Linear Circuit Analysis* (London, U.K.: Addison-Wesley, 1998) and *Complex Behavior of Switching Power Converters* (Boca Raton, FL: CRC Press, 2003), a coauthor of *Chaos-Based Digital Communication Systems* (Heidelberg, Germany: Springer-Verlag, 2003) and *Chaotic Signal Reconstruction with Applications to Chaos-Based Communications* (Singapore: World Scientific, 2007), and a coholder of a U.S. patent and two pending patents.

Dr. Tse was awarded the L. R. East Prize by the Institution of Engineers, Australia, in 1987, the IEEE Transactions on Power Electronics Prize Paper Award in 2001, and the International Journal of Circuit Theory and Applications Best Paper Award in 2003. In 2007, he was awarded the Distinguished International Research Fellowship by the University of Calgary, Canada. While with The Hong Kong Polytechnic University, he received twice the President's Award for Achievement in Research, the Faculty's Best Researcher Award, the Research Grant Achievement Award, and a few other teaching awards. From 1999 to 2001, he served as an Associate Editor for the IEEE TRANSACTIONS ON CIRCUITS AND SYSTEMS PART I-FUNDAMENTAL THEORY AND APPLICATIONS, and since 1999 he has been an Associate Editor for the IEEE TRANSACTIONS ON POWER ELECTRONICS. In 2005, he served as an IEEE Distinguished Lecturer. Presently, he also serves as the Editor-in-Chief of the IEEE CIRCUITS AND SYSTEMS SOCIETY NEWSLETTER, an Associate Editor for the IEEE TRANSACTIONS ON CIRCUITS AND SYSTEMS PART I-REGULAR PAPERS, the *International Journal of Systems Science*, the IEEE CIRCUITS AND SYSTEMS MAGAZINE and the *International Journal of Circuit Theory and Applications*, and a Guest Editor of a few other journals.